Shape Properties of Pulses Described by Double Exponential Function and Its Modified Forms

Gang Wu

***Abstract*—Double exponential function and its modified forms are widely used in high-power electromagnetics such as high-altitude electromagnetic pulse and ultrawide-band pulse study. Physical parameters of the pulse, typically the rise time t_r, full width at half maximum t_w, and/or fall time t_f, usually need to be transformed into mathematical characteristic parameters of the functions, commonly denoted as α and β. This paper discusses the dependences of pulse shape properties, represented by ratios of t_w/t_r and t_f/t_r, on a dimensionless parameter $A = \beta/\alpha$ or $B = \alpha/\beta$; and focuses on their limit correlations associated with the mathematical forms. It has been proven that pulses with $t_w/t_r <$ 4.29 cannot be expressed by the commonly used difference of double exponentials function. This limit can be mitigated partially by the latest proposed p-power of double exponentials function with a well-chosen p parameter. A novel form, difference of double Gaussian functions is also proposed to describe pulses with low t_w/t_r ratios better. Quotient of double exponentials, however, is shown to be the most flexible function for describing transient pulses with arbitrary t_w/t_r ratios, despite of its intrinsic drawbacks. All these functions are applied for several examples and further compared in both time and frequency domains.**

***Index Terms*—Difference of double exponentials (DEXP), difference of double Gaussian functions (DGF), high-altitude electromagnetic pulse (HEMP), p-power of double exponentials (PEXP), quotient of double exponentials (QEXP).**

I. Introduction

DOUBLE exponential function and its modified forms are widely used to describe high-power electromagnetic environments and their driven sources for simulation, such as high-altitude electromagnetic pulse (HEMP) [1]–[4] and ultrawide-band (UWB) pulses. For instance, difference of double exponentials (DEXP) and quotient of double exponentials (QEXP) have been used as a mathematical description of HEMP environments [1]–[4], as well as pulse shapes of the driven gamma-ray source in numerical simulations [5], [6]. A modified description, namely p-power of double exponentials (PEXP) has been proposed in recent years to improve the description of HEMP [2], lightning discharge [7], and near-filed electrostatic discharge environments [8]. Physical parameters of these EMP-like pulses, typically the rise time t_r, full width at half maximum (FWHM) t_w, and/or fall time t_f, usually need to be transformed with high precisions into mathematical characteristic parameters of the functions, commonly denoted as α and β. The least squares and Nelder–Mead algorithms have been applied for DEXP pulses to estimate the physical parameters from mathematical ones, and two complicated functions, sum of four exponential functions, are chosen to get approximate t_r and t_w values in a small ranging area of (α, β) [9], which cannot realize the inverse transform. Through numerical calculations and statistical means, novel correlations between the two groups of parameters, i.e., several sectional linear fit functions with gradational slopes between t_w/t_r, βt_w, and β/α, are established for a far-ranging area of (α, β) [10], [11]. As many as fifteen linear functions are formulated to express a correlation with typical overall fitting errors < 0.5% [11]. A limit property that a pulse shape can be fitted with DEXP function only for $t_w/t_r > 4.291$ has been noted [11], but without an explanation or a solution for pulses with lower t_w/t_r ratios.

This paper will discuss the dependences of the pulse shape properties, represented by ratios of t_w/t_r and t_f/t_r, on a dimensionless parameter $A = \beta/\alpha$ (or $B = \alpha/\beta$), and focus on the limit values of t_w/t_r and t_f/t_r ratios for the different aforementioned mathematical descriptions, as well as a newly proposed function, named as difference of double Gaussian functions (DGF). The mathematical description of pulses with lower t_w/t_r ratios will be also presented in variant forms and compared, which may be useful for expression of gamma-ray sources of some special nuclear weapons and UWB pulses.

II. Shape Properties of Variant Pulses

In general cases, the pulses concerned have unipolar waveforms increasing from zero to a maximum and then decreasing back to zero or almost zero, corresponding to real transient signals. The description function should be usually time-integrable, time-differentiable, convenient for analytical analysis, and better with a well-defined start time ($t = 0$). Fig. 1 shows a typical pulse shape $f(t)$, and definitions of several physical parameters to be used: t_p denotes the peak time at which the magnitude of $f(t)$ reaches its maximum value $f_{\max}$; t_1, t_2, t_3 on the rising edge, and t_6, t_5, t_4 on the falling edge, denote the time at which the magnitude equals to 10%, 50%, 90% of $f_{\max}$, respectively; $t_r = t_3 - t_1$ denotes a 10% to 90% rise time; FWHM $t_w = t_5 - t_2$; $t_f = t_6 - t_4$ denotes a 90% to 10% fall-time.

A. DEXP Pulses

The popular DEXP pulse has the form as

$$f(t) = k\left(\mathrm{e}^{-\alpha t} - \mathrm{e}^{-\beta t}\right)\ (t \geq 0) \quad (1)$$

Manuscript received July 15, 2013; revised September 22, 2013 and December 3, 2013; accepted December 4, 2013. Date of publication January 15, 2014; date of current version July 29, 2014.

The author is with the State Key Laboratory of Intense Pulsed Radiation Simulation and Effect, Northwest Institute of Nuclear Technology, 710024 Xi’an, China (e-mail: wugang00@gmail.com).

Color versions of one or more of the figures in this paper are available online at http://ieeexplore.ieee.org.

Digital Object Identifier 10.1109/TEMC.2013.2296573

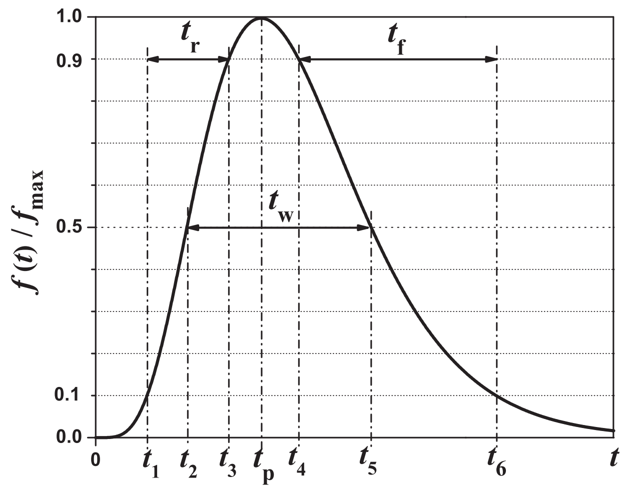

Fig. 1. Typical pulse shape and physical parameters commonly used for time-domain behavior.

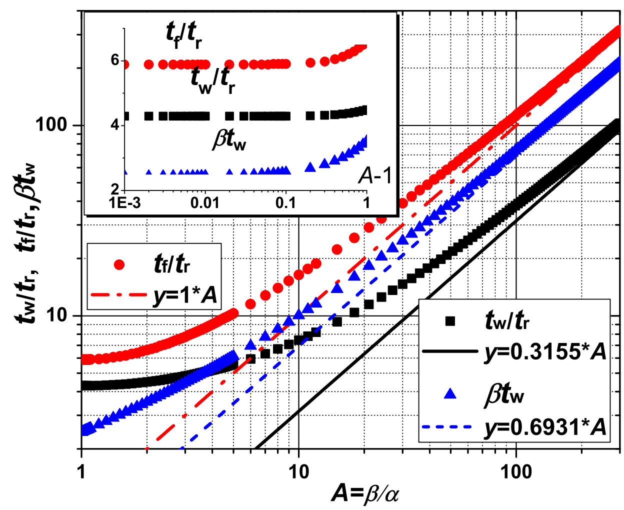

Fig. 2. $t_w/t_r, t_f/t_r$, and βt_w variations of DEXP pulses versus $A = \beta/\alpha$.

where $k = \beta e^{\alpha t_p} / (\beta - \alpha)$ is a normalized factor to make $f_{\max} = 1$, the peak time $t_p = [\ln(\beta/\alpha)] / (\beta - \alpha)$. The parameters α and β should satisfy the condition that $\beta > \alpha > 0$ to insure a positive polarity of $f(t)$.

For $\beta \gg \alpha$, the rise is much faster than the decay, we have

$$\begin{aligned}\beta t_r &= \beta(t_3 - t_1) \approx \ln 0.9 - \ln 0.1 = \ln 9\\ \alpha t_w &= \alpha(t_5 - t_2) \approx \alpha t_5 \cong \ln 2\\ \alpha t_f &= \alpha(t_6 - t_4) \approx \ln 9.\end{aligned}$$

Then, we can get that

$$\frac{t_w}{t_r} \approx \frac{\ln 2}{\ln 9} \cdot \left(\frac{\beta}{\alpha}\right) = 0.3155 \left(\frac{\beta}{\alpha}\right) \tag{2a}$$

$$\frac{t_f}{t_r} \approx \frac{\beta}{\alpha} \tag{2b}$$

$$\beta t_w = \alpha t_w \cdot \left(\frac{\beta}{\alpha}\right) \approx \ln 2 \cdot \left(\frac{\beta}{\alpha}\right) = 0.6931 \left(\frac{\beta}{\alpha}\right). \tag{2c}$$

Eq. (2a)–(2c) define three asymptotic linear limits of $t_w/t_r, t_f/t_r$, and βt_w as functions of a dimensionless parameter $A = \beta/\alpha$ for $A \gg 1$. This is the reason that $t_w/t_r, t_f/t_r$, and βt_w variations versus β/α appear as three straight lines in Fig. 2(a) of [11].

For $\beta/\alpha \to 1$, set $\beta/\alpha = 1 + \varepsilon, 0 < \varepsilon \ll 1$, (1) could be rewritten as

$$f(t) = k e^{-\alpha t} \left(1 - e^{-\alpha \varepsilon t}\right) \approx k e^{-\alpha t} \cdot \alpha \varepsilon t = k\varepsilon \cdot (\alpha t) e^{-\alpha t}$$

which means that the pulse shape is completely determined by the value of α, and the value of β only acts as a scaling factor through ε, since $k \to 1$ for $\varepsilon \to 0$.

Further set $\alpha t = x, g(x) = x e^{-x}$, we have $f(x) \cong k\varepsilon g(x)$. The maximum value of $g(x)$ is $g_{\max} = g(x = 1) = 1/e$. The transform of $\alpha t_i = x_i$ (i = 1–6) defines six dimensionless variables $x_1 \sim x_6$, and that (x_1, x_6), (x_2, x_5), and (x_3, x_4) are approximately the roots of the nonlinear equation $g(x) = c g_{\max} = c/e$ with the constant $c = 0.1, 0.5, 0.9$, respectively. Solving the equations numerically, we get

$$x_1 \cong 0.0382, x_6 \cong 4.8897; x_2 \cong 0.2320, x_5 \cong 2.6783;$$
$$x_3 \cong 0.6083, x_4 \cong 1.5318.$$

Further,

$$\frac{t_w}{t_r} \cong \frac{x_5 - x_2}{x_3 - x_1} = 4.2910 \tag{3a}$$

$$\frac{t_f}{t_r} \cong \frac{x_6 - x_4}{x_3 - x_1} = 5.8900 \tag{3b}$$

$$\beta t_w \cong \alpha t_w = 2.4463. \tag{3c}$$

This shows, that the lower limit of the DEXP equation corresponds to a ratio of t_w/t_r about 4.29, and t_f/t_r near 5.89. Pulses with lower ratios cannot be described in a good matter by DEXP. In that case, alternatives have to be found.

For general β/α values, set $A = \beta/\alpha, z = e^{-\alpha t}$, (1) can be transformed into a simple form as

$$f(z) = k\left(z - z^A\right)$$

and $k = A/z_p(A - 1)$, where $z_p = e^{-\alpha t_p} = A^{-\frac{1}{A-1}}$.

Then, let $z_i = e^{-\alpha t_i}, i = 1, \ldots, 6$, we have

$$\frac{t_w}{t_r} = \frac{\ln(z_2/z_5)}{\ln(z_1/z_3)}$$

$$\frac{t_f}{t_r} = \frac{\ln(z_4/z_6)}{\ln(z_1/z_3)}$$

$$\beta t_w = \alpha t_w \cdot (\beta/\alpha) = A \ln(z_2/z_5).$$

Note that (z_1, z_6), (z_2, z_5), and (z_3, z_4) are the roots of the nonlinear equation $f(z) = c f_{\max}$, i.e.,

$$z - z^A = c\left(1 - \frac{1}{A}\right) A^{-\frac{1}{A-1}} \tag{4}$$

with the constant $c = 0.1, 0.5, 0.9$, respectively. Apparently the roots only rely on the value of A, i.e., the ratio of α and β. (4) can be solved easily using iterative means. The results, as well as the asymptotic linear functions defined in (2a)–(2c) for

TABLE I
PARAMETER VALUES OF SECTIONAL LINEAR AND EXPONENTIAL FUNCTIONS TO FIT THE CORRELATIONS OF DEXP PULSES

$A=\beta/\alpha$	t_w/t_r			t_f/t_r			βt_w		
	s	y_0	%	s	y_0	%	s	y_0	%
→ 1	0	4.2910	-	0	5.8900	-	0	2.4463	-
[1.1, 3]	0.30247 (a) 2.445 (b)	3.80669	0.3	1.06402 (a) 2.44016 (b)	4.18377	0.8	-8.89667 (a) -6.65316 (b)	10.11291	0.2
[3, 10]	0.37659	3.68149	0.3	1.24167	4.0797	0.4	0.7938	2.14603	1.7
[10, 50]	0.35297	4.01636	1.3	1.1059	5.7273	2.1	0.72518	2.91094	1.3
[50, 300]	0.32468	5.69966	1.7	1.02324	10.52028	1.6	0.69926	4.36847	0.7
→ +∞	0.3155	0	-	1	0	-	0.6931	0	-

Linear function $y = sA + y_0$ is generally used, except for 1.1≤A≤3, exponential growth function $y = a\mathrm{e}^{A/\mathrm{b}} + y_0$ is introduced with values of a and b rather than s being given. '%' denotes maximum errors of estimation using the fit function in each section.

comparison, are shown in Fig. 2. The calculation distinguished from [11] is independent of the values chosen for α or β, making the results and discussions more general.

Numerical results shown in Fig. 2 confirm the asymptotic properties defined in (2a)–(2c) and the limit properties given in (3a)–(3c). The ratios, t_w/t_r and t_f/t_r, addressing major properties of pulse shapes, deviate from their own asymptotic linear functions more and more seriously as A decreases. In the range of $3 < A < 300$, several sectional linear functions, namely $y = sA + y_0$, are used to fit the correlations and for lower A values, an offset exponential growth function, $y = a\mathrm{e}^{A/b} + y_0$, is more adequate since there is a lower limit. Variations of βt_w versus $A = \alpha/\beta$ act as assistant variables to accomplish the transform between parameters (t_w, t_r) or (t_f, t_r) and $(\alpha,\ \beta)$. Parameter values of the fitting functions, with maximum errors of estimation using these functions in each section, are listed in Table I. The limit slopes given in (2a)–(2c), and lower limit values given in (3a)–(3c), are also tabulated. Compared to Table I of [11] for similar purpose, only three divided sections are used herein to cover a sufficient large range of A parameter, making the tabulation more practical for use.

B. QEXP Pulses

QEXP function has the basic form as

$$f(t) = k/(\mathrm{e}^{-\alpha t} + \mathrm{e}^{\beta t}) = k\mathrm{e}^{\alpha t}/\left(1 + \mathrm{e}^{(\alpha+\beta)t}\right) \tag{5}$$

where k is the normalized factor. Set $B = \alpha/\beta, z = \mathrm{e}^{-\beta t}$, (5) can be rewritten as

$$f(z) = k/\left(z^B + z^{-1}\right)$$
$$k = (1+B)/Bz_\mathrm{p}, z_\mathrm{p} = \mathrm{e}^{-\beta t_\mathrm{p}} = B^{-\frac{1}{B+1}}.$$

Description of a typical pulse with a rise fast compared to the decay requires $\alpha > \beta$, i.e., $B > 1$. For $\alpha = \beta$, or $B = 1$, it is a symmetric pulse that $t_f/t_r = 1$, and we can derive easily that $t_w/t_r = 1.04$.

The transform of $z_i = \mathrm{e}^{-\beta t_i}$ (i = 1–6) defines dimensionless variables $z_1 \sim z_6$, and that (z_1, z_6), (z_2, z_5), and (z_3, z_4) are roots of the following equation with the constant c = 0.1, 0.5, 0.9, respectively,

$$z^B + z^{-1} = k/c. \tag{6}$$

Apparently, these roots as well as variations of $t_w/t_r, t_f/t_r$, and αt_w concerned below, also rely only on the value of $B = \alpha/\beta$.

For $\alpha \gg \beta$, $B \gg 1$, we get $z_p \to 1, k \to 1$, (6) can be approximated as $z^B + z^{-1} \cong 1/c$. Then, we can determine the roots approximately through analytical analysis. The results are shown as follows

$$z_1 \cong 9^{1/B},\ z_6 \cong 0.1;$$
$$z_2 \cong 1,\ z_5 \cong 0.5;$$
$$z_3 \cong 9^{-1/B},\ z_4 \cong 0.9.$$

Further, we can get the correlations expressed as

$$\frac{t_w}{t_r} = \frac{\ln(z_2/z_5)}{\ln(z_1/z_3)} \cong B \cdot \frac{\ln 2}{2\ln 9} = 0.1577B \tag{7a}$$

$$\frac{t_f}{t_r} = \frac{\ln(z_4/z_6)}{\ln(z_1/z_3)} \cong 0.5B \tag{7b}$$

$$\alpha t_w = \beta t_w \cdot \left(\frac{\alpha}{\beta}\right) \cong B \cdot \ln 2 = 0.6931B. \tag{7c}$$

Eq. (7a)–(7c) demonstrate that $t_w/t_r, t_f/t_r$, and αt_w variations of QEXP pulses versus $B = \alpha/\beta$ are also characterized by three linear functions with given slopes when B is sufficiently large.

For $\alpha < \beta$, it can be similarly proven that there is a lower ratio limit for fitting pulses with a QEXP equation, determined as $t_w/t_r \to 0.3155$ corresponding to $\alpha \ll \beta$.

For general cases, we can solve (6) readily using iterative means. Numerical results for $B > 1$ cases, as well as the asymptotic linear functions defined in (7a)–(7c) for comparison, are shown in Fig. 3. Note that numerical results deviate from their own asymptotic linear functions markedly until the parameter B gets less than 200. To realize the transform between combined parameters (t_w, t_r) or (t_f, t_r) and $(\alpha,\ \beta)$ for practical use, several sectional linear functions, with their parameter values tabulated in Table II, are introduced to fit the correlations. Since there is no lower limit for these familiar cases, exponential growth functions are not necessary herein.

TABLE II
PARAMETER VALUES OF SECTIONAL LINEAR FUNCTIONS TO FIT THE CORRELATIONS OF QEXP PULSES

$B = \alpha/\beta$	t_w/t_r			t_f/t_r			αt_w		
	s	y_0	%	s	y_0	%	s	y_0	%
[1.1, 2]	0.32181	0.73432	0.6	0.70125	0.31018	0.5	1.13896	1.52643	0.6
[2, 8]	0.22347	0.93873	1.8	0.60549	0.51249	1.3	0.86972	2.11595	1.7
[8, 40]	0.17793	1.29105	1.0	0.54	1.03768	0.8	0.74174	3.10909	0.8
[40, 500]	0.16077	1.96126	0.9	0.50613	2.38379	0.7	0.69921	4.70139	0.5
$\to +\infty$	0.1577	0	-	0.5	0	-	0.6931	0	-

Linear function $y = sB + y_0$ is used; '%' denotes maximum errors of estimation using the fit function in each section.

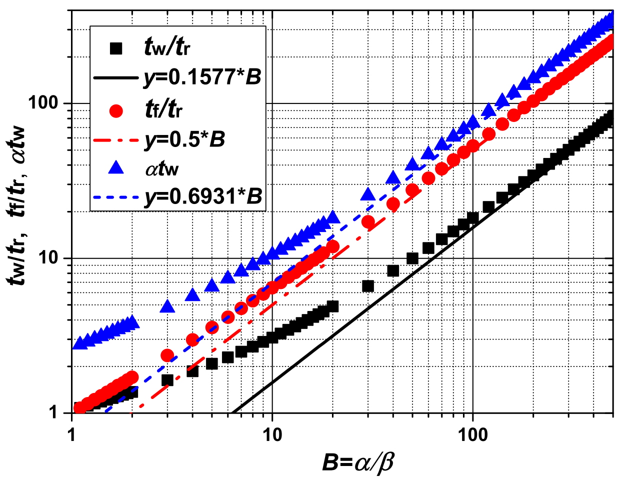

Fig. 3. t_w/t_r, t_f/t_r, and αt_w variations of QEXP pulses versus $B = \alpha/\beta$.

C. PEXP Pulses

PEXP function introduced in [2], [8] has the form as

$$f(t) = k(1 - \mathrm{e}^{-\alpha t})^p \mathrm{e}^{-\beta t} (t \geq 0, \alpha > 0, \beta > 0) \qquad (8)$$

where k is also a normalized factor to make $f_{\max} = 1$. Similar to QEXP functions, the rise edge mainly relies on the parameter α, whereas the fall edge mainly depends on the other one, and the condition $\alpha > \beta$ is not required to insure a positive polarity of $f(t)$.

For $\alpha \gg \beta$, we can deduce approximately that

$$1 - \mathrm{e}^{-\alpha t_1} \cong 0.1^{1/p}$$
$$1 - \mathrm{e}^{-\alpha t_3} \cong 0.9^{1/p}$$
$$\alpha t_r = \alpha (t_3 - t_1) \approx \ln \frac{1 - 0.1^{1/p}}{1 - 0.9^{1/p}}$$
$$\beta t_w = \beta (t_5 - t_2) \approx \beta t_5 \cong \ln 2$$
$$\beta t_f = \beta (t_6 - t_4) \approx \ln 9.$$

Choose $p = 2$ as a typical case, the analytical correlations can be established as following:

$$\frac{t_w}{t_r} \approx \frac{\alpha}{\beta} \ln 2 / \ln \frac{1 - 0.1^{\frac{1}{p}}}{1 - 0.9^{\frac{1}{p}}} = 0.2677 \frac{\alpha}{\beta} \qquad (9a)$$

$$\frac{t_f}{t_r} \approx \frac{\alpha}{\beta} \ln 9 / \ln \frac{1 - 0.1^{\frac{1}{p}}}{1 - 0.9^{\frac{1}{p}}} = 0.8485 \frac{\alpha}{\beta} \qquad (9b)$$

$$\alpha t_w = \beta t_w \cdot \frac{\alpha}{\beta} \approx \ln 2 \cdot \frac{\alpha}{\beta} = 0.6931 \frac{\alpha}{\beta}. \qquad (9c)$$

These show that asymptotic linear functions also exist for t_w/t_r, t_f/t_r, and αt_w variations of PEXP pulses versus $B = \alpha/\beta$ when B is sufficiently large.

For $\alpha \ll \beta$, set $\alpha/\beta = \delta \to 0$, (9) can be rewritten as

$$f(t) = k(1 - \mathrm{e}^{-\beta \delta t})^p \mathrm{e}^{-\beta t} \approx k\delta^p \cdot (\beta t)^p \,\mathrm{e}^{-\beta t}.$$

It implies that the pulse shape almost relies just on β.

Further defining $u = \beta t, h(u) = u^p \mathrm{e}^{-u}$, we get $f(u) \approx k\delta^p \cdot h(u)$. The maximum of the function $h(u)$ is determined as

$$h_{\max} = h(x = p) = p^p \mathrm{e}^{-p}.$$

The transform of $u_i = \beta t_i$ $(i = 1\text{–}6)$ defines dimensionless variables $u_1 \sim u_6$, and (u_1, u_6), (u_2, u_5), (u_3, u_4) are approximately roots of the following equation with the constant $c = 0.1, 0.5, 0.9$, respectively,

$$h(u) = u^p \mathrm{e}^{-u} = cp^p \mathrm{e}^{-p}. \qquad (10)$$

Roots of (10) depend only on the value of p parameter. Choosing $p = 2$, we get

$$u_1 = 0.2657,\ u_6 = 6.7292;\ u_2 = 0.7612,\ u_5 = 4.1559;$$
$$u_3 = 1.4191,\ u_4 = 2.7212.$$

Then, we deduce the limit properties as follows

$$\frac{t_w}{t_r} \cong \frac{u_5 - u_2}{u_3 - u_1} = 2.9432 \qquad (11a)$$

$$\frac{t_f}{t_r} \cong \frac{u_6 - u_4}{u_3 - u_1} = 3.4749 \qquad (11b)$$

$$\alpha t_w = \beta t_w \cdot \frac{\alpha}{\beta} \approx (u_5 - u_2) \cdot \frac{\alpha}{\beta} = 3.3947 \frac{\alpha}{\beta}. \qquad (11c)$$

These equations reveal that PEXP pulses should also have a rise fast compared to the decay, and for $p = 2$, the lower limits of t_f/t_r and t_w/t_r, about 3.47 and 2.94, respectively, are smaller than those of the DEXP pulses given in (3). If choosing larger p values, these lower limits can be further reduced with some extent. For $p = 5$, 10 and 20, the limits of t_f/t_r are 2.19, 1.74, and 1.48, respectively, whereas the limits of t_w/t_r are 2.17, 1.89, and 1.72, respectively. Note that for $p \geq 10$, the limit value of the fall time t_f tends to be smaller than the width t_w and description of pulses with $t_w/t_r < 1.72$ or $t_f/t_r < 1.48$ requires even larger p parameter. Comparing (11c) with (9c), it can be found that αt_w variations of PEXP $(p = 2)$ pulses versus

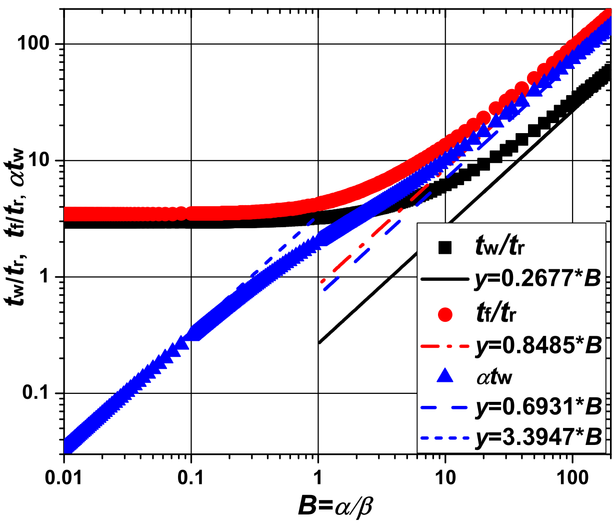

Fig. 4. t_w/t_r, t_f/t_r, and αt_w variations of PEXP ($p = 2$) pulses versus $B = \alpha/\beta$.

$B = \alpha/\beta$ are characterized by two asymptotic linear functions with given slopes for both $B \ll 1$ and $1 \ll B$ range.

For general α/β values, we can use similar transform as mentioned before. Set $B = \alpha/\beta, z = \mathrm{e}^{-\alpha t}$, (9) can be rewritten as

$$f(z) = k(1-z)^p z^{1/B}.$$

Further, we have

$$z_\mathrm{p} = \mathrm{e}^{-\alpha t_\mathrm{p}} = 1/(1+Bp)$$
$$k = (1+Bp)^{p+1/B}/(Bp)^p.$$

Let $z_i = \mathrm{e}^{-\alpha t_i}$, $i = 1$–6, (z_6, z_1), (z_5, z_2), (z_4, z_3) are the roots of the nonlinear equation $f(z) = c$, i.e.,

$$(1-z)^p z^{1/B} = c(Bp)^p/(1+Bp)^{p+1/B} \quad (12)$$

with the constant $c = 0.1, 0.5, 0.9$, respectively. Given the value of parameter p, these roots rely only on the parameter B.

Solving (12) numerically using iterative means, we can determine variations of t_w/t_r, t_f/t_r, and αt_w versus $B = \alpha/\beta$ through the following transform

$$\frac{t_w}{t_r} = \frac{\ln(z_2/z_5)}{\ln(z_1/z_3)}$$
$$\frac{t_f}{t_r} = \frac{\ln(z_4/z_6)}{\ln(z_1/z_3)}$$
$$\alpha t_w = \alpha(t_5 - t_2) = \ln(z_2/z_5).$$

Results of the calculation, for the parameter $p = 2$, as well as the asymptotic linear functions given in (9) and (11), are shown in Fig. 4. The results confirm the asymptotic and limit properties discussed above. For practical use of the correlations obtained to transform the parameters (t_w, t_r) or (t_f, t_r) to (α, β) or inversely, we also need several sectional linear and exponential growth functions to fit the data. Parameter values of these fitting functions are tabulated in Table III.

D. DGF Pulses

In order to describe pulses with low t_w/t_r or t_f/t_r ratios, we suppose to modify DEXP function by stretching the rise edge, and compressing the fall edge. We find naturally a DGF would be a choice, expressed as

$$f(t) = k\left(\mathrm{e}^{-\alpha^2 t^2} - \mathrm{e}^{-\beta^2 t^2}\right) \; (t \ge 0) \quad (13)$$

where k is a normalized factor to make $f_{\max} = 1$, and $\beta > \alpha > 0$ is required to keep $f(t)$ positive.

The function starts from zero at the defined $t = 0$ time, same as DEXP function, and clearly there is no discontinuity of the first derivative at the initial time since $f'(t = 0) = 0$.

The complete time integral of the function is given by

$$\int_0^{+\infty} f(\mathrm{t})\,\mathrm{dt} = \frac{k\sqrt{\pi}}{2}\left(\frac{1}{\alpha} - \frac{1}{\beta}\right) \quad (14)$$

which is also similar to the formulation for DEXP function.

For $\beta \gg \alpha$, the rise is much faster than the decay, we have

$$\beta t_\mathrm{r} = \beta(t_3 - t_1) \approx \sqrt{\ln 10} - \sqrt{\ln\left(\frac{10}{9}\right)}$$
$$\alpha t_\mathrm{w} \approx \alpha t_5 \approx \sqrt{\ln 2}$$
$$\alpha t_\mathrm{f} \approx \sqrt{\ln 10} - \sqrt{\ln\left(\frac{10}{9}\right)}.$$

Then, correlations can be established as follows

$$\frac{t_w}{t_r} \approx \frac{\beta}{\alpha} \cdot \sqrt{\ln 2} \Big/ \left(\sqrt{\ln 10} - \sqrt{\ln\left(\frac{10}{9}\right)}\right) = 0.6980\left(\frac{\beta}{\alpha}\right) \quad (15a)$$

$$\frac{t_f}{t_r} \approx \frac{\beta}{\alpha} \quad (15b)$$

$$\beta t_w = \alpha t_w \cdot \left(\frac{\beta}{\alpha}\right) \approx \sqrt{\ln 2} \cdot \left(\frac{\beta}{\alpha}\right) = 0.8326\left(\frac{\beta}{\alpha}\right). \quad (15c)$$

For $\beta/\alpha \to 1$, set $\beta^2/\alpha^2 = 1 + \varepsilon, 0 < \varepsilon \ll 1$, (13) can be rewritten as

$$f(t) = k\mathrm{e}^{-\alpha^2 t^2}\left(1 - \mathrm{e}^{-\varepsilon\alpha^2 t^2}\right) \approx k\varepsilon \cdot \alpha^2 t^2 \mathrm{e}^{-\alpha^2 t^2}$$

which reveals similarly that the pulse shape is almost determined by the parameter α, and the value of β only acts as a scaling factor through ε and k.

Further set $\alpha^2 t^2 = v, g(v) = v\mathrm{e}^{-v}$, we get $f(v) \cong k\varepsilon g(v)$. The six dimensionless variables $v_1 \sim v_6$, defined by the transform of $\alpha^2 t_i^2 = v_i$ $(i = 1$–$6)$, can be determined since (v_1, v_6), (v_2, v_5), and (v_3, v_4) are approximately the roots of the nonlinear equation $g(v) = cg_{\max} = c/\mathrm{e}$ with the constant $c = 0.1$, 0.5, 0.9, respectively. Solutions of an identical equation have been given in Section II-A, where they are denoted as x_i $(i = 1$–$6)$ and used to derive (3a) and (3b). The correlations herein should be written as

$$\frac{t_w}{t_r} \cong \frac{\sqrt{v_5} - \sqrt{v_2}}{\sqrt{v_3} - \sqrt{v_1}} = \frac{\sqrt{x_5} - \sqrt{x_2}}{\sqrt{x_3} - \sqrt{x_1}} = 1.9759 \quad (16a)$$

TABLE III
PARAMETER VALUES OF SECTIONAL LINEAR AND EXPONENTIAL FUNCTIONS TO FIT THE CORRELATIONS OF PEXP ($p = 2$) PULSES

$B=\alpha/\beta$	t_w/t_r			t_f/t_r			$B=\alpha/\beta$	αt_w		
	s	y_0	%	s	y_0	%		s	y_0	%
$\to 0$	-	2.9432	-	-	3.4749	-	$\to 0$	3.3947	0	-
[0.05, 2]	0.69001[(a)] 3.07021[(b)]	2.2385	0.6	1.71243[(a)] 2.64647[(b)]	1.71895	1.1	[0.05, 0.15]	2.92146	0.01446	1.7
							[0.15, 0.4]	2.31635	0.10902	1.9
							[0.4, 1]	1.67384	0.36881	1.9
							[1, 2]	1.22381	0.80877	1.0
[2, 10]	0.3092	2.98645	1.8	1.05118	3.22746	0.8	[2, 6]	0.91436	1.45638	1.9
[10, 40]				0.93461	4.48135	1.4	[6, 30]	0.75154	2.44539	1.6
[40, 200]	0.27745	4.30704	1.5	0.87249	7.37733	1.4	[30, 200]	0.70262	4.07091	1.4
$\to +\infty$	0.2677	0	-	0.8485	0	-	$\to +\infty$	0.6931	0	-

Linear function $y = sB + y_0$ is generally used, except for $0.05 \le B \le 2$, exponential growth function $y = ae^{B/b} + y_0$ is used for t_w/t_r and t_f/t_r, where values of a and b rather than s are given. '%' denotes maximum errors of estimation using the fit function in each section.

$$\frac{t_f}{t_r} \cong \frac{\sqrt{v_6}-\sqrt{v_4}}{\sqrt{v_3}-\sqrt{v_1}} = \frac{\sqrt{x_6}-\sqrt{x_4}}{\sqrt{x_3}-\sqrt{x_1}} = 1.6657 \quad (16b)$$

$$\beta t_w \cong \alpha t_w \cong \sqrt{v_5}-\sqrt{v_2} = \sqrt{x_5}-\sqrt{x_2} = 1.1549. \quad (16c)$$

This proves that DGF can be used to describe pulses with $t_w/t_r \ge 1.98$ or $t_f/t_r \ge 1.67$.

For general β/α values, set $A = \beta/\alpha, z = \mathrm{e}^{-\alpha^2 t^2}$, (13) can be rewritten simply as

$$f(z) = k\left(z - z^{A^2}\right)$$

where $k = A^2/z_\mathrm{p}\left(A^2-1\right), z_\mathrm{p} = \mathrm{e}^{-\alpha^2 t_\mathrm{p}^2} = A^{-\frac{2}{A^2-1}}$.

Then, let $z_i = \mathrm{e}^{-\alpha^2 t_i^2}, i = 1$–$6$, (z_1, z_6), (z_2, z_5), and (z_3, z_4) are the roots of the nonlinear equation $f(z) = c$, i.e.,

$$z - z^{A^2} = c\left(1 - \frac{1}{A^2}\right) A^{-\frac{2}{A^2-1}} \quad (17)$$

with the constant $c = 0.1, 0.5, 0.9$, respectively. Again, these roots rely only on the dimensionless parameter A.

Solving (17) numerically using iterative means, we can determine variations of t_w/t_r, t_f/t_r, and αt_w versus $A = \beta/\alpha$ through the following transform

$$\frac{t_w}{t_r} = \frac{\sqrt{-\ln(z_5)}-\sqrt{-\ln(z_2)}}{\sqrt{-\ln(z_3)}-\sqrt{-\ln(z_1)}}$$

$$\frac{t_f}{t_r} = \frac{\sqrt{-\ln(z_6)}-\sqrt{-\ln(z_4)}}{\sqrt{-\ln(z_3)}-\sqrt{-\ln(z_1)}}$$

$$\beta t_w = \alpha t_w \cdot (\beta/\alpha) = A\left(\sqrt{-\ln(z_5)}-\sqrt{-\ln(z_2)}\right).$$

Numerical results, as well as the asymptotic linear functions given in (15), are shown in Fig. 5. The results confirm the asymptotic and limit properties discussed above. Also, it can be seen that the asymptotic lines fit most data points so well, if using the asymptotic formulations to make estimations, errors of only a few percentage (<9.4%) would be introduced for all $A > 5$ cases. To fit the correlations with higher precision, we also just need quite a few sectional functions, as tabulated in Table IV.

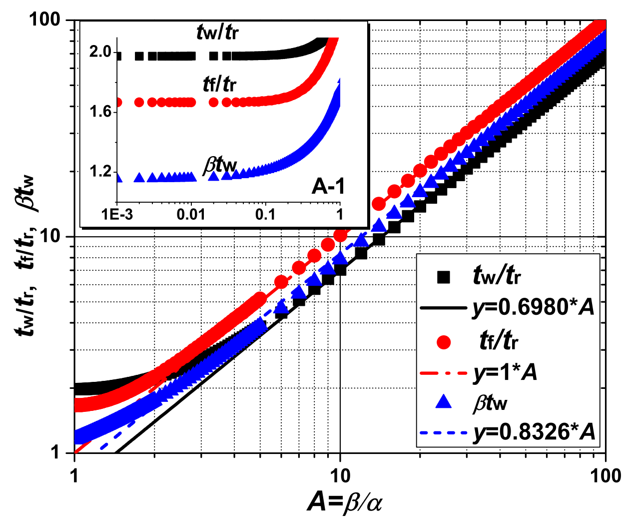

Fig. 5. t_w/t_r, t_f/t_r, and βt_w variations of DGF pulses versus $A = \beta/\alpha$.

Further considering pulses with $t_w/t_r < 1.97$ or $t_f/t_r < 1.66$, we suppose to modify DGF as following

$$f(t) = k\left(\mathrm{e}^{-\alpha^3 t^3} - \mathrm{e}^{-\beta^3 t^3}\right) \ (t \ge 0) \quad (18)$$

which is abbreviated as DMGF. The complete time integral of DMGF is given by

$$\int_0^{+\infty} f(\mathrm{t})\,\mathrm{d}t = \frac{k}{3}\Gamma\left(\frac{1}{3}\right)\left(\frac{1}{\alpha}-\frac{1}{\beta}\right). \quad (19)$$

where $\Gamma(z)$ is the Gamma function, and $\frac{1}{3}\Gamma\left(\frac{1}{3}\right) \cong 0.8930$.

We can derive easily that, limit correlations similar to (16) also exist for $\beta/\alpha \to 1$ cases, determined as

$$\frac{t_\mathrm{w}}{t_\mathrm{r}} \cong \frac{\sqrt[3]{x_5}-\sqrt[3]{x_2}}{\sqrt[3]{x_3}-\sqrt[3]{x_1}} = 1.5166 \quad (20a)$$

$$\frac{t_\mathrm{f}}{t_\mathrm{r}} \cong \frac{\sqrt[3]{x_6}-\sqrt[3]{x_4}}{\sqrt[3]{x_3}-\sqrt[3]{x_1}} = 1.0667 \quad (20b)$$

$$\beta t_\mathrm{w} \cong \alpha t_\mathrm{w} \cong \sqrt{x_5}-\sqrt{x_2} = 1.1549. \quad (20c)$$

These limit values are comparable to those of a single Gaussian function, which has a common shape property that $t_w/t_r =$

TABLE IV
PARAMETER VALUES OF SECTIONAL LINEAR AND EXPONENTIAL FUNCTIONS TO FIT THE CORRELATIONS OF DGF PULSES

$A=\beta/\alpha$	t_w/t_r			βt_w			$A=\beta/\alpha$	t_f/t_r		
	s	y_0	%	s	y_0	%		s	y_0	%
→ 1	-	1.9759	-	-	1.1549	-	→ 1	-	1.6657	-
[1.01, 3.3]	0.19057 [(a)] 1.73219 [(b)]	1.61531	1.3	5.08763[(a)] 9.87055[(b)]	-4.47446	0.06	[1.01, 1.6]	0.0057 [(a)] 0.38728 [(b)]	1.58375	0.4
[3.3, 10]	0.62498	0.75149	1.6	0.77499	0.04795	1.0	[1.6, 3.3]	0.89444	0.48294	1.2
[10, 100]	0.68306	0.22143	1.1	0.82982	-0.54969	1.3	[3.3, 100]	0.99868	0.17974	0.1
→ +∞	0.6980	0	-	0.8326	0	-	→ +∞	1	0	-

Linear function $y = sA + y_0$ is generally used, except for low A values, exponential growth function $y = ae^{A/b} + y_0$ is used with values of a and b rather than s being given. '%' denotes maximum errors of estimation using the fit function in each section.

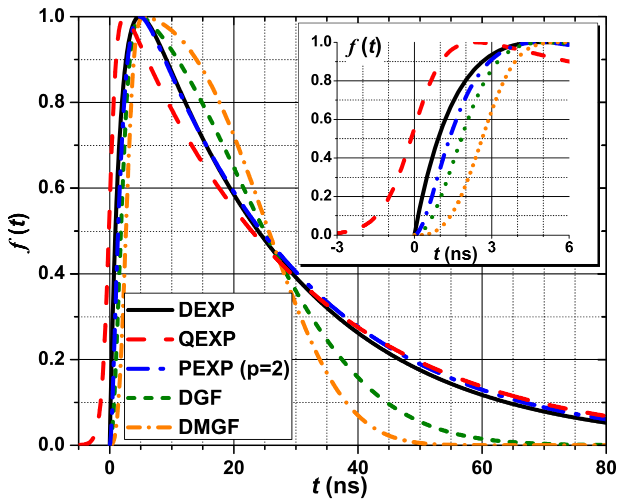

Fig. 6. Waveforms of the five variant descriptions tabulated in Table V.

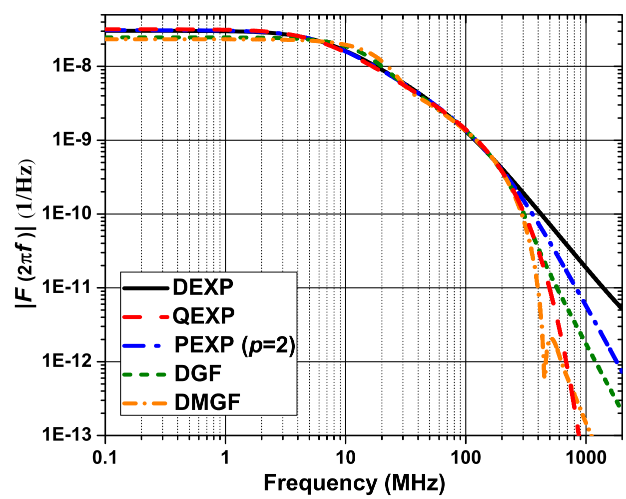

Fig. 7. Spectral magnitude of the waveforms in Fig. 6.

1.3959 and $t_f/t_r = 1$. However, DMGF pulses starts at $t = 0$ and are typically asymmetric since $t_f > t_r$.

It should be pointed out that, the Fourier transforms of DGF and DMGF are difficult to be expressed as analytical formulations, which may become a drawback for use if analytical analyses in frequency domain are needed. What we can determine analytically is the low frequency limits of their spectral magnitude through the complete time integrals given in (14) and (19).

III. VARIANT DESCRIPTIONS OF A STANDARD PULSE

To check the usability of DGF and DMGF, and validate the effectiveness of the transform relation tabulated in Tables I–IV, we use variant functions discussed above to describe a standard pulse, with a rise time of $t_r = 2.5$ ns and FWHM of $t_w = 23$ ns, which has been widely known as the key waveform feature of early time (E1) HEMP environment. Parameter values of these functions are determined through the linear transform relations listed, with an identical procedure that calculating the dimensionless parameter $A = \beta/\alpha$ or $B = \alpha/\beta$ via slope and intercept values fitting t_w/t_r correlations, then substituting this parameter to solve αt_w or βt_w, and further α and β. The results are listed in Table V. t_r and t_w values of these functions, characterized by the determined mathematical parameters, are also calculated and given. The fact that the error amounts less than one percent for both these two parameters indicates that the transform relations established are effective for use.

TABLE V
PARAMETER VALUES OF VARIANT FUNCTIONS DESCRIBING A STANDARD PULSE ($t_r = 2.5$ NS, $t_w = 23$ NS)

	DEXP	QEXP	PEXP (p=2)	DGF	DMGF
α/s^{-1}	4.02×10^7	1.57×10^9	7.63×10^8	3.43×10^7	3.47×10^7
β/s^{-1}	5.90×10^8	3.49×10^7	3.80×10^7	4.50×10^8	3.36×10^8
k	1.307	1.114	1.268	1.036	1.0087
t_r/ns	2.50	2.51	2.48	2.53	2.50
t_w/ns	23.01	22.99	23.06	23.10	23.00
t_f/ns	54.89	62.96	57.93	33.67	24.14
$\int_0^{+\infty} f(t)dt$ / ns	30.34	31.86*	31.08	24.77	23.29
$\int_0^{+\infty} f^2(t)dt$ /ns	17.30	16.96*	17.21	16.93	17.53

* For QEXP, the integrals start from $t = -\infty$.

The fall times, complete time integrals of variant functions, and their squares are also listed for comparison. It can be seen that these three features of DEXP, QEXP, PEXP ($p = 2$) descriptions are very close. The proposed DGF and DMGF descriptions have much smaller fall times than the other three functions, as their temporal variations are more localized. However, their complete time integrals, representing the impulse of the transient if electromagnetic stress signals are described, are much closer to the other three, with discrepancies less than 3 dB

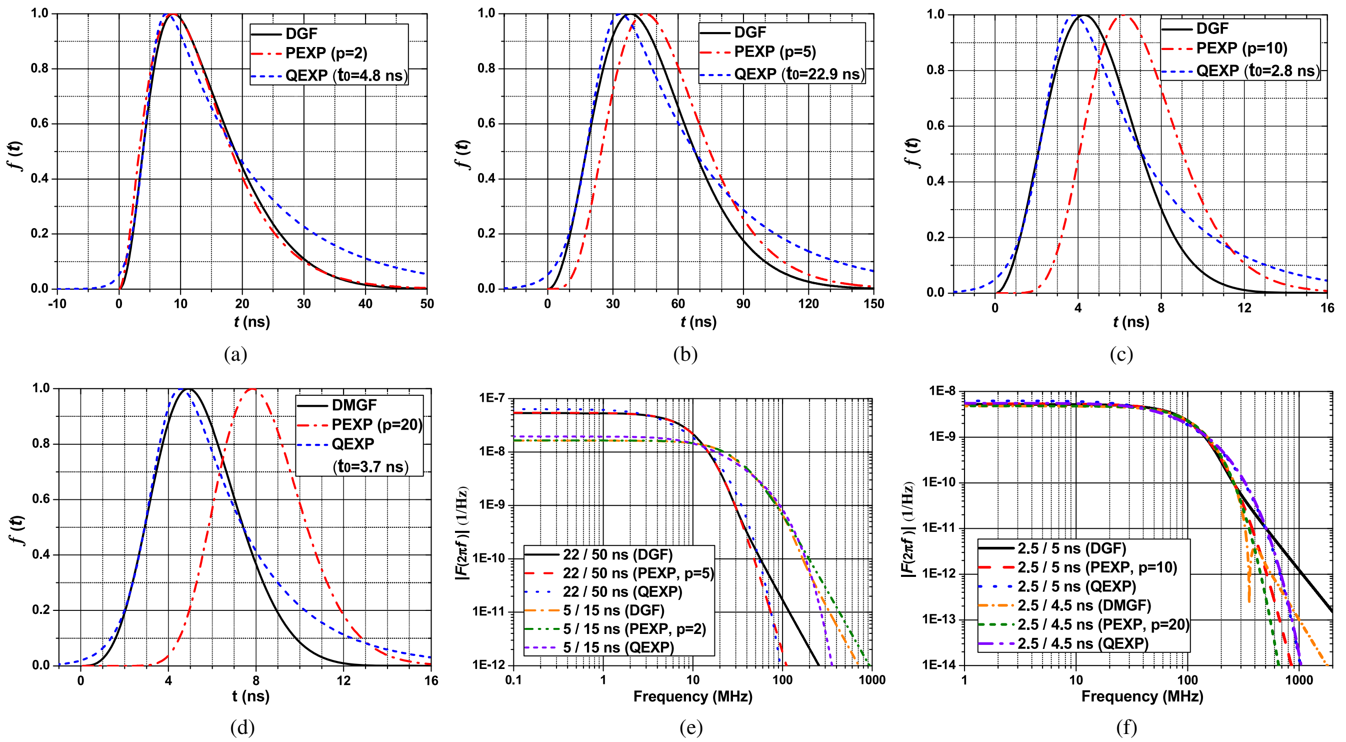

Fig. 8. Variant mathematical descriptions of pulses with low t_w/t_r ratios listed in Table VI (a) $t_r = 5$ ns, $t_w = 15$ ns, $t_w/t_r = 3$(b) $t_r = 22$ ns, $t_w = 50$ ns, $t_w/t_r = 2.27$(c) $t_r = 2.5$ ns, $t_w = 5$ ns, $t_w/t_r = 2$(d) $t_r = 2.5$ ns, $t_w = 4.5$ ns, $t_w/t_r = 1.8$(e) Spectral magnitude of pulses in (a)–(b) (f) Spectral magnitude of pulses in (c)–(d).

and the time integrals of the squares, typically representing the energy of the transient, are almost identical.

The time-domain waveforms and frequency domain spectral magnitude of the five variant descriptions are illustrated in Figs. 6 and 7. It can be seen that DEXP and PEXP ($p = 2$) waveforms in the time domain are almost superposed, despite for a very bit discrepancy during the rise edge. DGF has a rise behavior similar to these two functions, whereas the rise edge of DMGF is rather slower and similar to that of QEXP function. The fall edges of the five functions deviate more apparently. Their frequency domain spectral magnitude, however, have much less diversities in the main range of 0.1–250 MHz, with discrepancies less than 3 dB. Significant differences appear in higher frequency ranges above 300 MHz, that the DEXP function has the largest magnitude, secondarily PEXP ($p = 2$), whereas high frequency spectra of DGF and DMGF are closer to QEXP. Note that there is a singular sharp dig, near 450 MHz, on the spectral magnitude of DMGF, which appears to be a singularity of the spectral magnitude function, and may limit its usage.

IV. Descriptions of Pulses with Low τ_w/t_r Ratios

Real transient signals may have arbitrary waveforms that pulses with low t_w/t_r ratios should be also properly dealt with in simulations of threat environments and their effects. For instance, a real UWB pulse may have a rise time of 200 ps and FWHM of 400 ps, i.e., $t_w/t_r = 2$. In HEMP (E1) environment calculation, variant gamma-ray pulses should be considered to check the factors highly affecting the results. [12] has

TABLE VI
Parameter Values of Variant Functions Describing Pulses with Low t_w/t_r Ratios

No.	t_r/ns	t_w/ns	t_w/t_r	Function	α/s^{-1}	β/ s^{-1}	k
1	5	15	3	QEXP	6.82×10^8	7.11×10^7	1.367
				PEXP (p=2)	6.11×10^7	1.75×10^8	26.88
				DGF	5.28×10^7	1.88×10^8	1.35
2	22	50	2.27	QEXP	1.46×10^8	2.47×10^7	1.513
				PEXP (p=5)	2.27×10^7	6.45×10^7	1.695×10^2
				DGF	1.73×10^7	3.65×10^8	1.989
3	2.5	5	2	QEXP	1.24×10^9	2.70×10^8	1.598
				PEXP (p=10)	2.17×10^8	7.73×10^8	2.478×10^3
				DGF	2.08×10^8	2.60×10^8	6.141
4	2.5	4.5	1.8	QEXP	1.20×10^9	3.25×10^8	1.678
				PEXP (p=20)	1.79×10^8	1.17×10^9	2.586×10^6
				DMGF	1.44×10^8	2.63×10^8	1.7097

mentioned several representative physical parameters of simultaneous gamma-ray pulses radiated from different-type nuclear weapons. We estimate t_r values from t_2, t_3 parameters and cite directly t_w parameters given in the literature, as listed in the first three rows in Table VI. To further extend t_w/t_r ratios lower than 2, a fourth case, i.e., $t_r = 2.5$ ns, $t_w = 4.5$ ns, $t_w/t_r = 1.8$, is artificially added to make only DMGF, PEXP ($p = 20$), and QEXP functions suitable for describing it.

Using the correlations tabulated in Tables I–IV, parameters of variant mathematical descriptions suitable for each pulses, are determined and given in Table VI. Time domain waveforms and spectral magnitude of these descriptions are illustrated in Fig. 8. Note that QEXP pulses are properly shifted along the time axis to match the rise edges of DGF pulses for comparison.

As shown in Fig. 8(a), DGF and PEXP ($p = 2$) descriptions of a $t_w/t_r = 3$ pulse almost superpose in the time domain, and there is only a quite small discrepancy (3–4 dB) at high frequency ranges (>200 MHz) between their spectral magnitude curves shown in Fig. 8(e).

For pulses with even lower t_w/t_r ratios, as shown in Fig. 8 (b)–(d), five-, ten-, and 20-power PEXP functions are needed for use, with the result that the whole wave shapes are postponed later and later. Though the functions still start from zero at the initial time, the zero-to-peak (0%-100%) rise time tends to be increased a lot, which significantly limits their spectral magnitude in high frequency ranges even lower than QEXP pulses. Besides, the fact that the normalized factor k grows so rapidly, with a variation of five magnitudes as t_w/t_r decreasing from 3 to 1.8, implies this type of function may become gradually ineffective for describing these pulses with much lower t_w/t_r ratios.

DGF pulses still have whole wave shapes quite close to PEXP ($p = 5$ and $p = 10$) for $t_w/t_r = 2.27$ and 2 pulses, and the main rise edges also quite close to those of QEXP descriptions. Their spectral magnitude at high frequency ranges, however, become larger than those of PEXP ($p = 5$ or 10) and QEXP pulses, whereas the discrepancies of these three descriptions in the main spectral range (less than 50 MHz and 600 MHz for both cases, respectively) are quite small. For a pulse with $t_w/t_r = 1.8$, as illustrated in Fig. 8(d), DMGF rather than DGF, should be used, which remains to hold similar wave shape to PEXP ($p = 20$) and similar main rise edge to QEXP, as well as very close spectral magnitude to them below 200 MHz. Again, a singular sharp dig, near 350 MHz herein, still appears on the curve, corresponding to the singularity of the Fourier transform function. However, this will not restrict its use for expressing a gamma-ray pulse since only time-domain behaviors are concerned.

V. Conclusion

In this paper, correlations between key physical parameters and mathematical parameters for pulses described by double exponential function and its modified forms are established, in order to transform them each into the other.

Pulse shape properties, represented by ratios of t_w/t_r and t_f/t_r, are proven to rely only on the dimensionless parameter $A = \beta/\alpha$ (or $B = \alpha/\beta$). It is a common feature that for sufficiently large A (or B) values, t_w/t_r and t_f/t_r ratios of all five functions mentioned all scale proportional to A (or B) values but with different slopes. Another common feature emphasized greatly is that all of DEXP, PEXP, and the newly proposed DGF/DMGF have lower limits on t_w/t_r and t_f/t_r ratios for sufficiently small A (or B) values.

The widely used DEXP function is suitable only for pulses with $t_w/t_r > 4.29$ and $t_f/t_r > 5.89$. PEXP ($p = 2$) function is suitable for pulses with $t_w/t_r > 2.94$ and $t_f/t_r > 3.47$, and the pulse shape for large t_w/t_r ratios approaches quite close to that of DEXP while cancelling the drawback, discontinuity of the first derivative at the initial time. Higher-power PEXP has further lower limits on these ratios, but the whole pulse shape should be postponed a lot, limiting the rise edge quite longer and the spectral magnitude at high frequency range much lower. DGF is proposed to describe pulses with low t_w/t_r ratios, but still only suitable for $t_w/t_r > 1.98$. The modified form, DMGF, can further reduce the limits of t_w/t_r, t_f/t_r to 1.51 and 1.07, respectively, despite of the singular point appearing on the spectral magnitude curve. QEXP is found to be the most flexible function for describing EMP-like transient pulses with arbitrary t_w/t_r ratios, though the pulse shape may need to be properly time shifted, or an artificial initial time is well chosen.

Example applications for four pulses, with t_w/t_r ranging from 1.8 to 3, illustrate that all these functions have quite accordant spectral magnitude curves in the main frequency range, despite of obvious discrepancies in the higher frequency range.

Acknowledgment

The author would like to thank the reviewers for their careful review and valuable suggestions. The author also thanks to the colleague, Dr. C. Mao for some useful discussions.

References

[1] Electromagnetic Compatibility (EMC)—Part 2: Environment—Section 9: Description of HEMP Environment—Radiated Disturbance, IEC 61000-2–9 Ed. 1.0, 1996–2002. [Online]. Available: www.iec.ch

[2] Y. Xie, "A modified description of early time high-altitude electromagnetic pulse waveform (E1)," Sensor and Simulation Note 562, Univ. New Mexico, Albuquerque, NM, USA , Jan. 2013.

[3] C. E. Baum, "Some considerations concerning analytic EMP criteria waveforms," Theoretical Note 285, Air Force Weapons Lab., Kirtland Air Force Base, Albuquerque, NM, USA, Oct. 1976.

[4] C. E. Baum, "From the electromagnetic pulse to high-power electromagnetics ," System Design and Assessment Note 32, Univ. New Mexico, Albuquerque, NM, USA, 1991.

[5] C. L. Longmire, R. M. Hamilton, and J. M. Hahn, " A nominal set of high-altitude EMP environments ," Theoretical Note 354, Air Force Phillips Lab., Kirtland Air Force Base, Albuquerque, NM, USA, Jan. 1987.

[6] K.-D. Leuthäuser, "A complete EMP environment generated by high altitude nuclear bursts: Data and standardization," Theoretical Note 364, Air Force Phillips Lab., Kirtland Air Force Base, Albuquerque, NM, USA, Feb. 1994.

[7] F. Zhang, Y. Chen, M. Wei, and S. Liu, "Representing the lightning current by pulse function," *Chinese J. Radio Sci.*, vol. 17, no. 1, pp. 51–53, Feb. 2002.

[8] Z. Yuan, T. Li, J. He, S. Chen, and R. Zeng, "New mathematical descriptions of ESD current waveform based on the polynomial of pulse function," *IEEE Trans. Electromagn.Compat.*, vol. 48, no. 3, pp. 589–591, Aug. 2006.

[9] M. Camp and H. Garbe, "Parameter estimation of double exponential pulse (EMP, UWB) with least squares and Nelder Mead algorithm," *IEEE Trans. Electromagn. Compat.*, vol. 46, no. 4, pp. 675–678, Nov. 2004.

[10] C. Mao, X. Guo, H. Zhou, and Y. Xie, "Fitting method of the simulated HEMP waveform by the double-exponential function," *High Power Laser Particle Beams*, vol. 16, no. 3, pp. 336–340, 2004.

[11] C. Mao and H. Zhou, "Novel parameter estimation of double exponential pulse (EMP, UWB) by statistical means," *IEEE Trans. Electromagn. Compat.*, vol. 50, no. 1, pp. 97–100, Feb. 2008.

[12] J. Wang, S. Niu, D. Zhang, and D. Qiao, *Effect Parameter Handbook of High Altitude Nuclear Detonation*. Beijing, China: Atomic Energy Press, 2010, pp. 108–109.

Gang Wu was born in Wuhan, China, in June, 1982. He received the B. Eng. degree in nuclear engineering and nuclear technology, and the Ph.D. degree from Tsinghua University, Beijing, China, in 2004 and 2010 respectively.

His research interests include: high-altitude electromagnetic pulse environment, effect, and testing methods; pulsed X-ray sources and system-generated electromagnetic pulse.